J Neurophysiol 89: 450–459, 2003;
10.1152/jn.00053.2002.

Using Arm Configuration to Learn the Effects of Gyroscopes and Other Devices

MARTHA FLANDERS, JAN M. HONDZINSKI, JOHN F. SOECHTING, AND JADIN C. JACKSON
Department of Neuroscience, University of Minnesota, Minneapolis Minnesota 55455

Submitted 28 January 2002; accepted in final form 20 September 2002

Flanders, Martha, Jan M. Hondinski, John F. Soechting, and Jadin C. Jackson Using arm configuration to learn the effects of gyroscopes and other devices. *J Neurophysiol* 89: 450–459, 2003; 10.1152/jn.00053.2002. Previous studies have perturbed the association between motor commands and arm movements by applying forces to the arm during two-dimensional movements. These studies have revealed that, when the normal hand path is perturbed, subjects gradually adapt their motor commands to return to this path. The present study used the spin of a gyroscope to create a complex perturbation, as subjects reached to targets presented in three dimensions. Hand path did not change, but the whole-arm geometry ("arm configuration" in four dimensions) was altered. Over a series of several hundred reaches to various targets, subjects gradually returned the arm movement to its normal configuration. Furthermore, during the course of this learning, subjects used a strategy that involved manipulating arm posture. A similar strategy was observed when subjects made reaching movements with a rod attached to the upper arm to change its inertial characteristics. In both cases, the gradual return to the normal arm movement was accomplished without an increase in kinetic energy, suggesting that arm postures and movements (kinematics) and muscular forces (kinetics) may be mutually optimized. In contrast to previous studies, the present results highlight the role of arm configuration (rather than hand path) in learning and control.

INTRODUCTION

Moving or manipulating an object is facilitated by prior experience with its mechanical properties. For example, a bottle is lifted differently depending on whether it is empty or full, and this difference can be prepared in advance of the movement. The present investigation sought an answer to the following question: What strategy does the sensorimotor system use to develop a representation of the mechanics of devices held in the hand or placed on the arm?

The shape and mass distribution of a hand-held object, as well as the geometric configuration of the arm, appear to be important sensorimotor parameters. Based on psychophysical studies of object manipulation, Turvey and colleagues (1999) concluded that the somatosensory system is "attuned" to the object's inertial geometry. They proposed that, during active manipulation, sensation of the object's volume is important for controlling the level of muscle activation, and sensation of the object's symmetry is important for controlling the pattern of muscle activation (Shockley et al. 2001). Even when there is no object in the hand, inertial geometry plays a critical role in sensorimotor control. For example, in studies of arm reaching movements in two dimensions (2D), Ghez and colleagues (1990) showed that patients lacking proprioception fail to appropriately compensate for the fact that the arm's posture-dependent inertial resistance to movement is an anisotropic function of force direction (see also Buneo et al. 1995).

Whereas many early studies of reaching were done with the arm supported in the horizontal plane (the plane containing the shoulder joint), the arm's inertial geometry may be even more fundamental to the control of free reaching. Soechting and colleagues (1995) showed that, when moving the hand between pairs of initial and final three-dimensional (3D) target locations, the variation in the final arm configuration could be accounted for by assuming that subjects choose the movement that encounters minimal inertial resistance. In a free-reaching movement, various sequences of arm posture are possible, even if the hand is moved along a straight line. We found that subjects tend to favor the relatively low-inertia, humeral rotation axis rather than shoulder flexion or abduction (Soechting et al. 1995). In related studies, we showed that, in generating these movements, the arm motor system tends to minimize kinetic energy (dynamic force) rather than potential energy (antigravity force) or total energy (dynamic force + antigravity force) (Nishikawa et al. 1999; Soechting and Flanders 1998). Naturally, we wondered how free-reaching movements adapt to changes in inertial geometry or to unusual dynamic forces.

Many previous studies of 2D reaching (reviewed under DISCUSSION) had shown that subjects adapt to perturbed hand trajectories by gradually returning the hand to its normal straight-line path. An underlying assumption appeared to be that the error signal driving the learning was related to hand-path curvature or endpoint error. In contrast, in the present study we created a situation in which the reach was not constrained to 2D, and a subtle dynamic perturbation influenced the series of postures traversed by the moving arm, but not the hand-path curvature or the endpoint error. If the goal of motor learning is to return the hand to its normal path, there should be no adaptation in this situation. However, we found significant adaptation, apparently aimed at returning the whole-arm movement to its normal geometric configuration.

Address for reprint requests: M. Flanders, Department of Neuroscience, 6–145 Jackson Hall, 312 Church St. S.E., University of Minnesota, Minneapolis MN 55455 (E-mail: fland001@umn.edu).

The costs of publication of this article were defrayed in part by the payment of page charges. The article must therefore be hereby marked "*advertisement*" in accordance with 18 U.S.C. Section 1734 solely to indicate this fact.

METHODS

Overview

The main experiment involved a spinning gyroscope held in the hand (GYRO); the second experiment involved a long rod (ROD) attached to the upper arm to change its inertia. In both experiments subjects started with the arm by the side (the "standard location," SL), reached the hand up to an "initial" target location (usually location 12, as described below), and then reached over to a "final" target location (e.g., location 1). In the ROD experiment each successive reaching movement was from target 12 to target 1 (the subject then returned to the SL and briefly rested between trials). In the GYRO experiment, the reach from target 12 to target 1 was followed by several other reaches to other targets throughout the workspace. Subjects were unaware that the final analysis would focus only on the reaches from target 12 to target 1; the reach of interest ("12 to 1," as justified below) was embedded in a somewhat complex manner, in various sets of eight reaching movements.

The basic experimental design followed a standard learning paradigm. Figure 1 illustrates the sequence of experimental conditions for the ROD experiment (Fig. 1*B*) and the GYRO experiment (Fig. 1, *A* and *C*). The ROD experiment simply consisted of 20 sequential 12-to-1 reaches without perturbation (NORM), 40 sequential 12-to-1 reaches with a ROD on the arm, and then 30 more NORM trials. In the GYRO experiment, the sets of 8 reaches were performed under three sequential conditions; 8 sets of 8 were NORM, 24 sets of 8 were GYRO/MASS, and then 32 sets of 8 were GYRO/MASS + SPIN. These conditions involved reaching *1*) while holding a grip with a short pen as a pointer (NORM), *2*) with a gyroscope (or gyro) attached to the grip/pen (GYRO/MASS), and then *3*) with the gyroscope spinning (GYRO/MASS + SPIN, or SPIN). During the latter two conditions, subjects were expected to learn the mechanical properties of the added mass and/or spin by gradually adapting the brain's mapping between motor commands and the resulting movements.

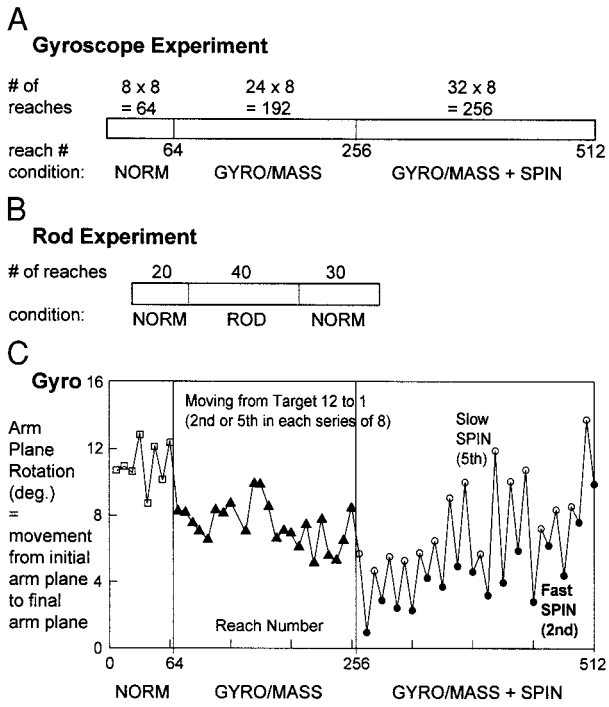

FIG. 1. Experimental design. *A*: in the gyroscope experiment, the reach between a particular target pair occurred once in each 8-reach series. The subject first reached normally (NORM), then reached while holding a gyroscope (GRYO/MASS), then reached with the gyro spinning (GYRO/MASS + SPIN). There were 8 series in the NORM condition, 24 series in the GYRO/MASS condition, and 32 series in the GYRO/MASS + SPIN condition. *B*: in the rod experiment, 20 normal reaching movements (NORM) were followed by 40 ROD trials and then 30 NORM trials. *C*: in the gyroscope experiment, subjects started at the standard posture (angle of arm plane approximately 0°) and reached through 64 series of 8, for a total of 512 reaches. The rotation of the arm plane during movements from target 12 to target 1 is plotted for subject 1; this target pair was alternated into the second and fifth spot in each successive series. Since the gyroscope was charged at the start of each series, the spin was faster at the beginning than at the end. Thus the spin had a greater influence on the movement when this target pair was second (filled circles) rather than fifth (open circles) in the 8-target series.

Instructions to subjects: GYRO experiment

All subjects (in both experiments) gave informed consent in accordance with the policies of the University of Minnesota human subjects committee. In the GYRO experiment, eight naive subjects reached to a series of targets placed in a 3D workspace by a robot arm. The robot indicated a target location and then quickly moved to another target location as the subject held the hand in the first location. When the robot stopped at a target location, a tone cued the subject to start the reach. The robot held the target in place during the reach, and subjects had full view of this target (a sphere, 3.5-cm diam).

During each movement, the subject held a lightweight grip with an 8-cm-long pen extending forward as if it were the subject's finger. The pen tip was to be placed just in front of the target sphere; there were no constraints on speed or accuracy. A foam mold of the gyro was replaced by the real (0.4 kg) gyro during the transition from the normal reaching task (NORM condition) to the GYRO/MASS condition. For the GYRO/MASS + SPIN condition, the gyro's spin axis was forward, or anterior when the arm was in the standard posture (see Fig. 2*A*). The inertia around the spin axis was 6.05×10^{-5} kg·m^2 and its maximum angular velocity was 785 rad/s. For the reach from 12 to 1, the maximum effect of the torque due to the spin was about 10% of the maximum joint torque in shoulder elevation and elbow flexion and about 1% of the maximum joint torque in shoulder yaw and humeral rotation (see Fig. 3).

Sixty-four times in each GYRO experiment, the subject began in a standard initial posture, made a series of eight reaching movements, and then briefly rested. In the SL the upper arm was approximately vertical and the forearm was horizontal, in a parasagittal plane (Fig. 2*A*). So that the movements covered the entire 3D workspace, we used most of the 18 target locations described in our previous study (for exact locations see Soechting et al. 1995). Some of these locations are shown schematically in Fig. 2*B* (viewed from behind the subject) and in Fig. 2*A* (viewed from the side with targets 12 and 3 out of the page and targets 16 and 7 into the page). The first movement was from the standard posture to target 12 or to target 3. The sequence of presentation of subsequent target pairs was then varied within each series, and it typically took the hand back and forth and up and down across the workspace, visiting targets at two different distances from the shoulder. For example, in one series the hand moved from the SL to 12 to 1 to SL to 3 to 5 to 6 to 14 to 7. In another series, the hand moved from SL to 3 to 5 to SL to 12 to 1 to 16 to 2 to 9. Thus the 12-to-1 reach was alternated into the second or fifth location in a series and always followed a reach from the standard location.

Design considerations: GYRO experiment

We surmounted a number of design considerations in the GYRO experiment. First, as mentioned above, the design featured a relatively large number of movements between two particular target pairs: 12-to-1 and 3-to-5 were each presented once per eight-trial series. These pairs were chosen because preliminary simulations showed that the spin of our gyroscope should maximally perturb movements with these particular geometries. In reach 12-to-1, the hand moved 54 cm, from the upper right to the upper left quadrant of the workspace (Figs. 2*B* and 4*A*). Target 3 was 10 cm distal to 12, and target 5 was 53 cm directly forward from the shoulder (Fig. 2*A*). We alternated reach

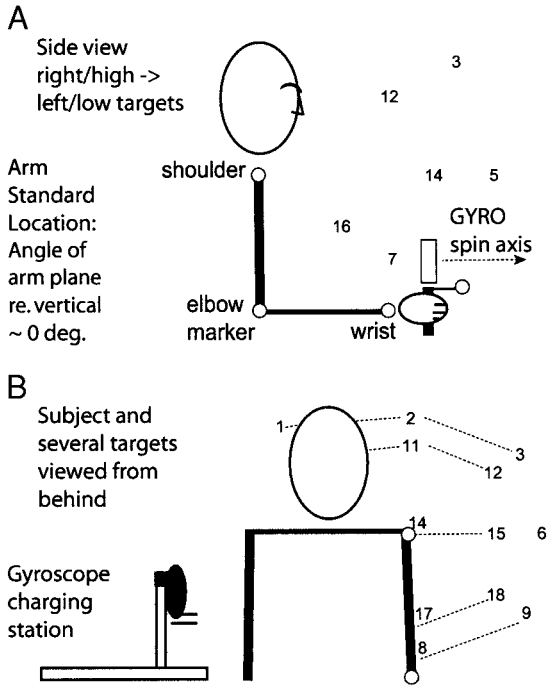

FIG. 2. Schematic view of the subject, the gyroscope, the gyroscope charging station, and some of the targets. *A*: the 8-reach series began with the arm in a standard location (arm plane nearly vertical). Targets 14 and 5 were straight ahead from the shoulder; targets 12 and 3 were upward and to the subject's right; targets 16 and 7 were downward and to the subject's left. *B*: the subject is viewed from behind and some of the targets are hidden by the body. The charging station was to the subject's left at approximately the same anterior/posterior level as the trunk.

12-to-1 and reach 3-to-5 into the second and fifth place in the eight-trial set.

The gyroscope itself was custom designed with three goals: *1*) it needed to be light and portable enough so that subjects could easily adapt to the GYRO/MASS, *2*) the spin had to have sufficient momentum to perturb a reach, and *3*) the device needed to be devoid of vibration. Due to these constraints, it was not possible to mount the motor on the handle and it was instead placed on a table to the left of the subject (see Fig. 2*B*). At the beginning of each eight-reach series in the GYRO/MASS + SPIN condition, the subject activated the gyroscope by attaching it to the motor. The gyro device was held in the subject's normal right-hand grip during charging, but the handle was horizontal. When fully charged, the device was detached from the motor and rotated into the upright position as it was moved across the lower body to the standard location. Once in this standard posture, the subject was prepared to make the series of eight reaches. The spin produced a very complex pattern of perturbation as it was rotated into the starting location, and there was no perturbation when the gyro device was held stationary.

Because the motor was not mounted on the device, the rate of spin gradually decreased. Since the magnitude of the torque contributed by the spinning gyro was proportional to the angular velocity of the spin, this unfortunately resulted in a gradually decreasing magnitude of perturbation. The angular velocity was initially set to 785 rad/s but had decreased to about 628 rad/s by the second reach and to about 512 rad/s by the fifth reach. To illustrate this phenomenon, in Fig. 1*C*, we have extracted kinematic data from the 12-to-1 reach (a total of 64 trials) across the entire series of 512 (64 × 8) reaches (from one subject). It is apparent that there was a difference in the effect of the gyroscope's spin, depending on whether the 12-to-1 reach was the second (filled circles) or the fifth (open circles) in each eight-reach series. In the results section, we therefore track the time course of adaptation by extracting data for a particular target pair each time it was the second in the sequence (see Fig. 4). Thus the 32-trial time course in Fig. 4 actually corresponds to 512 sequential reaches to a wide range of targets.

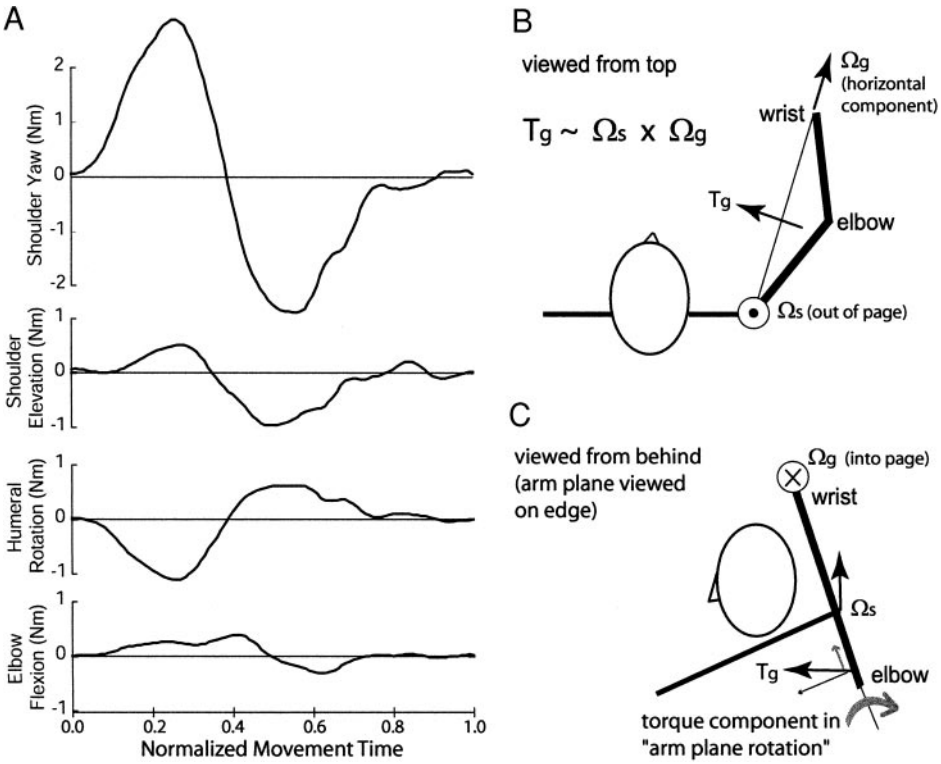

FIG. 3. *A*: joint torque computed from normal reaching movements from target 12 to target 1. *B–C*: a highly simplified schematic to illustrate the kinds of torques (Tg) that may be caused by moving (with a shoulder rotation, Ωs) a spinning gyroscope (Ωg). In *B*, the subject is viewed from above, with the plane formed by the shoulder, elbow and wrist (the arm plane) about 20° from vertical. In *C*, the perspective is such that the arm plane is viewed on edge. There is a component of the gyro's torque in the arm plane. (Assume the right-hand rule in interpreting the torque and rotation axes.)

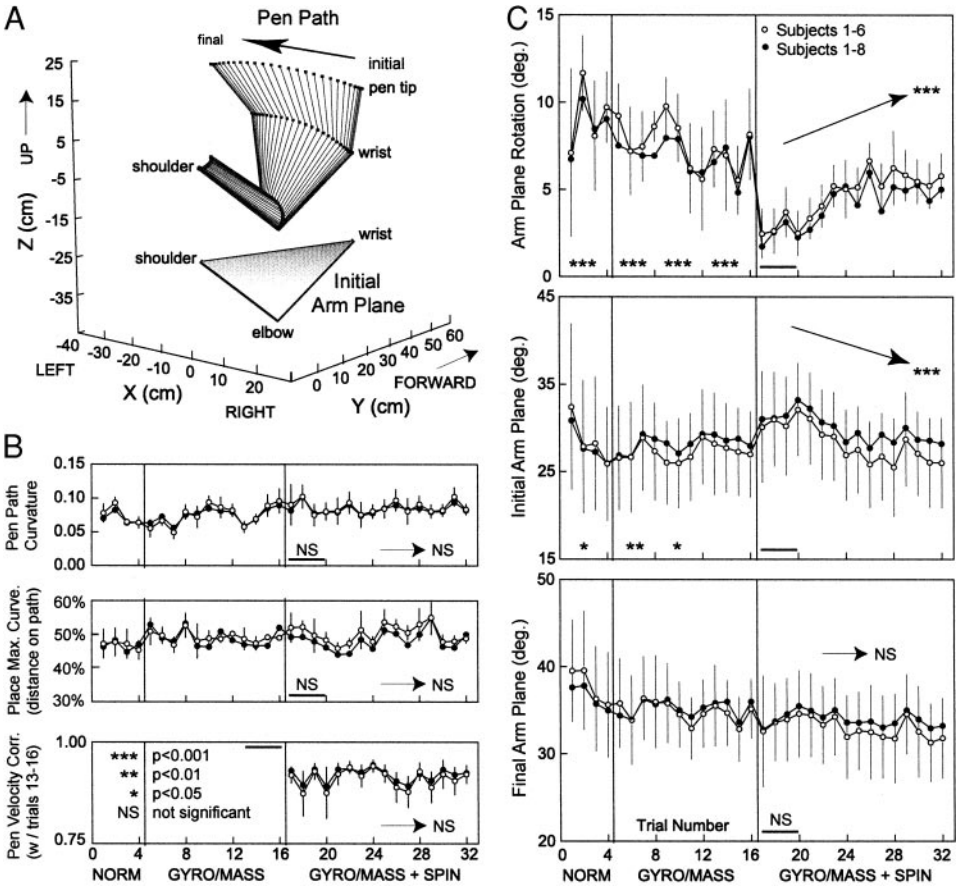

FIG. 4. The spin of the gyroscope resulted in changes in arm posture but not pen path. *A*: stick figures formed by the shoulder, elbow, wrist and pen tip provide a three-dimensional view of the movement (drawn from samples taken at 30 Hz) from target 12 to target 1 (see Fig. 2*B*). The "Arm Plane" is the plane containing the shoulder, elbow and wrist; its spatial orientation changes during the movement. The spatial orientation of this plane is quantified as the angle that it makes with a vertical plane. *B*, Three parameters related to the 3D trajectory of the "Pen Path" did not change across trials. Each point represents a movement from target 12 to 1, when it was presented second in the series of 8. For the velocity correlation method (*bottom panel*) each data point represents the average correlation of the SPIN trial with each of the last four CONTROL trials (13–16). *C*: two of the three parameters related to arm posture showed changes when the gyroscope was set in motion (the GYRO/MASS + SPIN condition, trials 17–32). Most notably, the spatial orientation of the initial arm plane moved from about 26 to 32° (i.e., to a more horizontal inclination) and then back down to about 26° (*middle panel*). Subjects 1–6 (open circles) showed a greater degree of adaptation than the full set of 8 subjects (filled circles). In *B* and *C*, the four trial groups marked by lines and stars were significantly different from each other; those marked as NS were not (ANOVA, Tukey HSD posthoc testing). Arrows indicate the results of linear regressions across trials in the SPIN condition. Error bars indicate standard error of the mean of subjects 1–6. All other statistics refer to pooled data from subjects 1–8.

Design and subjects: ROD experiment

In a second experiment, we used a different type of perturbation for comparison with results of the GYRO experiment. We changed the mass distribution of the arm by connecting two collinear rods (each 21 cm long, 1.2 cm in diameter, and 0.23 kg) to the upper arm in the anterior and posterior directions (with the arm in the standard posture). The choice of rod ("ROD") parameters was based on preliminary simulations. (Interestingly, the simulations showed that it is relatively difficult to significantly alter the geometrical properties of the arm inertia without restricting movement or substantially increasing mass.) On each consecutive trial, the 6 subjects began at the standard posture and then reached from target 12 to 1. In this ROD experiment, the maximum effect of the perturbation was more substantial than for the GYRO experiment; it amounted to about 25%, 20% and 5% of the peak torques in shoulder elevation, humeral rotation and shoulder yaw, respectively, and 0% at the elbow.

Data acquisition and analysis

In the ROD experiment, the *xyz*-locations of magnetic sensors on the shoulder, elbow and wrist were recorded at 40 Hz using a Polhemus Fastrak system. Pen path was not recorded in this experiment.

In the gyroscope experiment, we used a 4-camera system from Motion Analysis, Co. The three-dimensional locations of 6 passive markers were recorded at 60 Hz. Subjects wore a wrist brace to prevent wrist flexion/extension, and we found that wrist pronation/supination was negligible for target pair 12 to 1 ($<1^o$ supination). Therefore arm posture was completely described by the *xyz*-locations of the wrist (or pen tip) and the spatial orientation of a plane containing the upper arm and forearm (the "arm plane" in Figs. 4*A*). The orientation of the arm plane (with respect to vertical) was computed from the locations of the shoulder, elbow and wrist markers (Soechting et al. 1995). By convention, 0^o refers to a vertical arm plane and 90^o refers to a horizontal arm plane.

For the second major target pair featured in the design of the gyroscope experiment (3 to 5), subjects consistently exhibited about 3^o of pronation during the reach. As described under Results, we found that subjects manipulated and adapted the arm plane rotation in a manner similar to that observed for the target pair 12 to 1. Unfortunately, however, with this additional degree of freedom, we were not able to accurately simulate the mechanics. Thus although the subjects' strategy appeared to be similar, we cannot provide a full analysis, and the Results section will focus on movements from target 12 to 1.

The trajectory of the pen tip was quantified in three ways. First, as a standard measure of path curvature, we computed (in 3D) the maximum deviation from a straight-line path and divided it by the length of the straight-line path (Nishikawa et al. 1999). Next, we resampled the pen path at 100 equidistant points and determined the place of maximum curvature as a percentage of path length. Finally, we adapted the velocity correlation method of Shadmehr and Mussa-Ivaldi (1994) for use in 3D. This method compared the 3D pen velocity vector at each point during a movement to the corresponding vectors for the CONTROL movements in trials 13–16 (see Fig. 4*B*).

The tangential velocity profile of the wrist marker was used to judge movement onset, end, and a "half-way" point, which was defined as the point of maximum velocity. Peak kinetic energy (KE_p) was then computed at the point of maximum wrist velocity. The general form of the equation is

$$KE_p = \tfrac{1}{2} m v^2 + \tfrac{1}{2} \Omega^T \times I\Omega$$

where m is the mass of the arm, v is the velocity of the center of mass, Ω is the joint angular velocity vector and I is the inertia tensor. To examine the influence of arm geometry on kinetic energy we com-

puted a "normalized kinetic energy" by dividing the peak kinetic energy for a particular trial by the peak velocity squared (of the wrist marker).

Estimating mechanical effects

During a free reaching movement, the arm's acceleration and deceleration unfold across time in several degrees of freedom. Therefore it impossible to guess, or even to fully intuit the mechanical effects of the gyroscope or the rod. Basically, the rod alters the mass and the moment of inertia of the arm, whereas the spin of the gyroscope provides no resistance to translation, but a velocity-dependent resistance to attempts to rotate the spin axis.

As shown in Fig. 3*A*, reaches from 12 to 1 are produced by joint torques in four degrees of freedom: shoulder yaw, shoulder elevation, humeral rotation, and elbow flexion. The movement resulting from these torques depends on the inertia of the arm, which differs widely across the various axes of rotation, and changes with arm posture. In Figs. 3*B* and 3*C*, a stick figure is drawn with the arm held up (at target 12), and with the arm plane having a spatial orientation of about 20°. Ignoring elbow rotation, the torque due to the spin of the gyro (Tg) is proportional to the vector cross product of the shoulder's rotational velocity (Ωs) and the gyro's spin axis (Ωg) (Fig. 3*B*). (The torque, Tg, is zero when the arm is stationary.) For reach 12 to 1, adduction (positive yaw) is the largest component of shoulder rotation. In Fig. 3*B*, we have therefore drawn the Ωs axis as coming out of the page, and we have drawn only the horizontal component of the gyro's spin axis (Ωg). As shown in Fig. 3*C*, during the reach, the torque due to the gyro's spin (Tg) was therefore horizontal; it had a component perpendicular to the arm plane, tending to move the hand downward, and a component in the arm plane, tending to move the elbow inward (gray arrows). As mentioned above, the movement due to Tg will depend on the rotational inertias along the various axes, which change with arm configuration. Thus it is impossible to intuit the effect, and it must instead be calculated.

To estimate the effect of the perturbation in various arm configurations, we conducted a series of computer simulations. Our approach was to pose the following question: What would be the initial mechanical effect of the perturbation if the subject were to produce the same joint torques as used under CONTROL conditions? Thus we based the simulations on the computed torques for an adapted GYRO/MASS trial (for the gyroscope experiment) or for a representative NORM trial (for the rod experiment).

Simulations were performed using Matlab (The MathWorks) and Maple (Waterloo Maple). We used the *x*,*y*,*z*-joint locations recorded for each reach, to compute angular joint positions, velocities, and accelerations. First, experimental data were reduced to *xyz*-coordinates of the elbow and wrist with respect to the shoulder. These data were then resampled at 200 Hz, transformed into joint angles and low-pass filtered at 5 Hz. As shown in Fig. 3*A*, we computed joint torques (shoulder yaw and elevation, humeral rotation, and elbow flexion) for the entire movement (Craig 1989). The parameters of the arm were then modified to include the perturbation of choice (i.e., SPIN or ROD) and the new initial conditions (i.e., the new initial posture). These parameters were used with the original torques to integrate and predict the new arm movement.

These simulations and calculations were checked in two ways: first, the LaGrangian method was compared against the iterative link method (Craig 1989) for computing joint torques to insure proper formulas; second, the simulations were run using unaltered arm parameters to confirm that movement trajectories were unaltered.

When examining mathematically complex systems with multiple parameters, it can be instructive to vary a single parameter while holding all other variables fixed. Since our subjects appeared to be varying their initial arm posture, in our simulations we varied the postural and inertial properties of the arm while holding the joint torques fixed. In this way, we hoped to estimate the mechanical effect of the perturbations and to understand how changing initial arm posture might compensate or aggravate such an effect.

Several assumptions were made. Since previous studies have demonstrated that dynamics are preferentially optimized, the quasi-static anti-gravity torques were ignored (Soechting et al. 1995; Nishikawa et al. 1999). Additionally, the equations of motion assumed no friction or velocity dependent damping; and, where the gyro was concerned, the gyro's rotor was assumed not to slow down appreciably during a given trial (i.e., a single reach). Finally, the spatial location of the shoulder was fixed.

The simulation was based on a hypothetical scenario where the subject approached a perturbed trial planning to produce the same set of joint torques as used for unperturbed trials; we ignored reflexive and other short-latency reactions to the applied torques. Previous (two-dimensional) simulations (Shadmehr and Brashers-Krug 1997; Buneo et al. 1995) have established that this is a reasonable approach for simulating mechanical effects only in the first half of the movement, since the simulated movements based on this scheme will not come to a stop.

For reaching to targets in 3D, the movement is fully characterized by the *xyz*- location of the hand and the spatial orientation of the arm plane. In the sections below, we will show that hand path was not altered (this will be presented in Fig. 4*B*). Thus to avoid the complex multidimensional display used in Fig. 3, we will simplify the representation of mechanical effects to one degree of freedom: the rotation of the spatial orientation of the arm plane across time (the "arm path"), in the first half of the reach (see Fig. 5*A* and Fig. 6*C*).

RESULTS

Kinematic adaptation to the spinning gyroscope

The main experiment was designed to apply a subtle gyroscopic perturbation to otherwise natural reaching movements. Human subjects started in a standard arm posture (Fig. 2*A*) and were asked to reach through several series of 8 targets, in locations that covered the three-dimensional (3D) workspace (Fig. 2*B*). Target order was varied, but the experimental design focused on two particular target pairs: targets 3 to 5 and targets 12 to 1. These two target pairs were presented either second or fifth in each sequence of 8, and were always preceded by a reach from the standard arm posture. Due to friction, the gyroscope gradually decreased its rate of spin during each 8-trial series. Therefore subsequent analyses were focused on the trials with the fastest spin (see METHODS).

Due to conservation of angular momentum, a spinning gyroscope resists changes in its spin axis. The most dramatic effect of this perturbation was on the rotation of the plane of the arm during the movement. This is shown in Fig. 1*C* for one subject (fast and slow spin trials) and in the top panel of Fig. 4*C* for all subjects (fast spin trials only). In contrast, hand path did not change (Fig. 4*B*). We used three methods for quantifying the trajectory of the hand in 3D space (the "Pen Path" in Fig. 4*A*). We then performed an ANOVA and posthoc tests to compare each group of four consecutive trials to the values of the first four trials in the SPIN condition (marked by small horizontal lines in the top two panels of Fig. 4*B*). The pen path did not change significantly in the SPIN condition. In the case of the velocity correlation method, correlations (with the last four trials of the GYRO/MASS condition) remained high and constant throughout the SPIN condition.

As explained under METHODS, we measured the spatial orientation of the plane formed by markers on the shoulder, elbow and wrist (the "Arm Plane" in Fig. 4*A*), to characterize arm

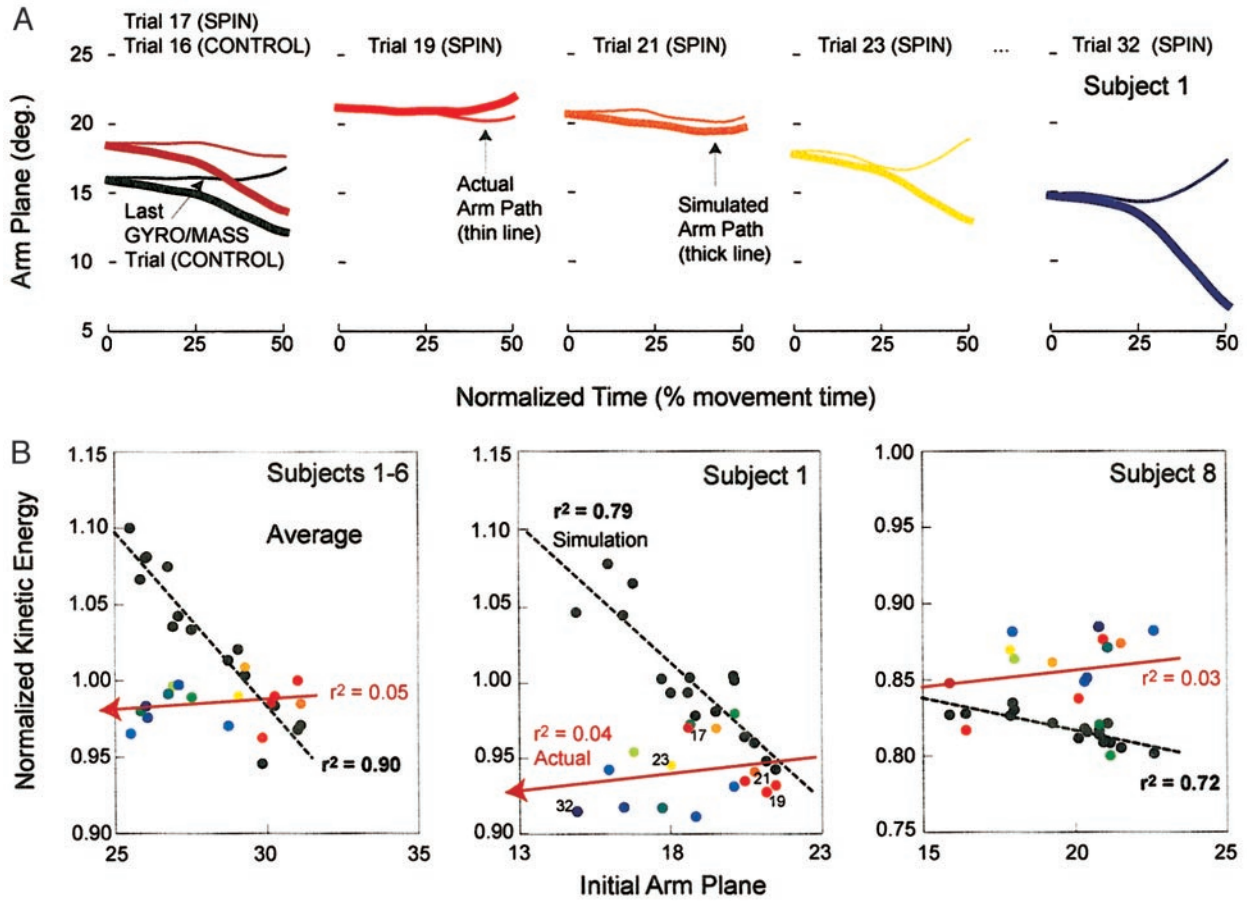

FIG. 5. A kinetically ideal initial posture for coping most easily with the spin of the gyroscope. We computed the joint torques for the last trial of the CONTROL condition and then used them to examine the effect of changing the initial posture. *A*: rotation of the arm plane (the "arm path") during the first half of the movement. The thin lines represent the actual movements of subject 1; the thick lines represent the simulated mechanical effect of the spin. The black lines represent the CONTROL trial and the dark red lines represent the first trial of the SPIN condition. The subject experienced a relatively unperturbed movement in trials 19–21 by adopting a more horizontal initial posture. He then returned to the normal arm path in trials 23–32, and avoided a potentially large perturbation by adapting his muscular forces. *B*: averaged data from subjects 1–6, data from subject 1, and the less representative data of subject 8. If subjects used the torques from the CONTROL condition, decreasing the initial arm plane would correspond to a higher level of normalized kinetic energy (black circles and dotted lines). Subjects did change the initial posture on successive trials (red = early, yellow/green = middle, blue = late) but did not increase kinetic energy.

configuration. We performed ANOVA and posthoc tests to compare each group of four consecutive trials to the values of the first four trials in the SPIN condition. We found that the spin of the gyro was associated with significant changes in the initial arm plane (*middle panel*, Fig. 4*C*) and in the rotation of the arm plane, i.e., amount of movement from the initial arm plane to the final arm plane (*top panel*, Fig. 4*C*). The amount of arm plane rotation dropped at the beginning of the SPIN condition. However, the change in initial arm plane was not as immediate as the change in arm plane rotation. The orientation of the initial arm plane increased its value (i.e., becoming more horizontal) and then retuned to the control (GYRO/MASS) values. Final arm plane did not change as markedly as these other two arm plane parameters.

To further quantify the changes in all kinematic parameters across the SPIN condition, we preformed a linear regression analysis. Linear regression across trial means in the SPIN condition showed that arm plane rotation ($r^2 = 0.62$) and initial arm plane ($r^2 = 0.52$) gradually changed toward the normal values (see arrows in Fig. 4*C*, $P < 0.001$). In contrast, the other parameters did not change significantly (NS).

As mentioned under METHODS, the reach from 3 to 5 exhibited consistent pronation, and we therefore focus on data from the movement between target 12 and target 1. However, ignoring pronation, we found that subjects manipulated and adapted the arm plane rotation in a manner similar to that observed for the target pair 12 to 1. The analogous ANOVA and posthoc tests on arm plane rotation showed that the first four SPIN trials were different from all NORM and GYRO/MASS trials, as well as the last four SPIN trials ($P < 0.05$).

Returning to the reach from target 12 to 1, the statistical analysis presented above was based on pooled data from the 8 subjects (filled symbols in Fig. 4). However we noticed that two of the subjects showed very little perturbation by or adaptation to the spin of the gyro (open symbols in Fig. 4 exclude these two subjects). Linear regression across arm plane rotation for SPIN trials supported this impression, revealing r^2 values of 0.04 and 0.10 ($P > 0.20$) for subjects 7 and 8, respectively.

According to physical principles, one possible way to avoid being perturbed by the spin would be to increase self-generated torques, i.e., to move more quickly. This is due to the fact that

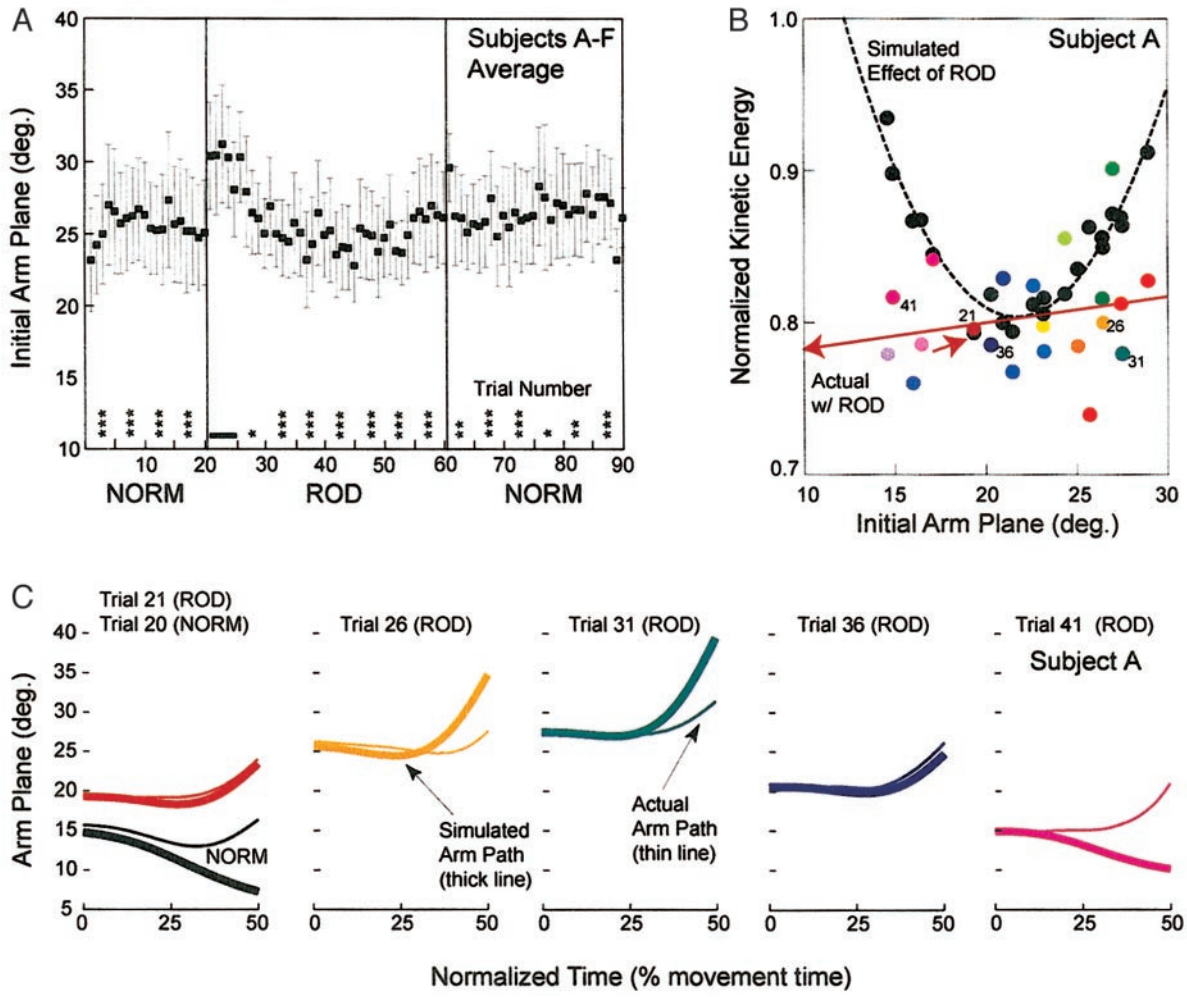

FIG. 6. A kinetically ideal initial posture for reaching (from 12 to 1) with a rod on the upper arm. Sequential conditions were: without the rod (NORM), with the rod (ROD) and then without the rod again (NORM). *B* and *C*: early ROD trial numbers 21–41 are color coded progressively as red, orange/yellow, green/blue, purple, and then pink. *A*: a more horizontal initial arm plane was adopted when the rod was initially attached to the arm. A significant change was revealed using ANOVA on consecutive blocks of 5 trials, with pooled data from 6 subjects (asterisks represent significance levels as defined in Fig. 4). Error bars indicate standard error of the mean of subjects A-F. *B*: simulations showed that the mechanical effect of the rod was a quadratic function of initial posture (black symbols and dotted line), with an ideal initial arm plane that corresponded to a state visited during the course of adaptation (e.g., trials 21 and 36 for subject A, colored symbols). *C*: as subject A increased his initial arm plane from trial 21 to 26 and 31, the mechanical effect of the perturbation reversed (thick lines). He then returned to the ideal posture in trial 36, before adopting the normal initial posture in trial 41. In trial 41 and beyond, an elevation in kinetic energy and a large perturbation could only by avoided by using a new pattern of muscular forces.

self-generated torques increase with velocity squared (Atkeson and Hollerbach 1985), whereas torques due to the gyro are proportional to the spin angular velocity. Thus moving the arm more quickly would make the torques attributable to the spin relatively less important. Subjects generally did not use this strategy during the course of adaptation: movement time (average = 969 ms) remained constant across SPIN trials in all subjects except subject 6 (linear regression for each subject at $\alpha = 0.05$). Interestingly, however, Subjects 7 and 8 had the shortest movement times of all of the subjects (average = 864 and 814 ms, respectively) and therefore may have been relatively insensitive to the perturbation.

Analysis of mechanical effects

Thus the subjects who were perturbed and adapted generally did so not by changing the hand path or the movement speed, but by changing the orientation of the initial arm plane and the amount of rotation of the arm plane. Our simulations (see METHODS) suggested an interpretation for this phenomenon. In Fig. 5 we show that the mechanical effect of the spin would change with initial arm posture if subjects continued to use the same pattern of joint torques as used in the last trial of the GYRO/MASS condition (CONTROL trial).

Figure 5*A* features data from subject 1; the results are representative of subjects 1–6. The plots depict the spatial orientation of the arm plane across time (the "arm path") during the first half of the movement (0–50% of the movement time; approximately 500 ms). Actual movements (thin lines) are compared with simulated movements (thick lines) for the CONTROL trial (16) and five SPIN trials (17, 19, 21, 23 and 32). During the first half of the CONTROL trial, the angle of the arm plane increased (thin black line). If the subject used the

same joint torques and the same starting posture, the effect of the spin would be to push the arm plane in the opposite direction (thick black line). In trial 17 (dark red lines), the subject used a slightly different initial posture and the movement (thin line) was indeed perturbed in the direction of the simulated mechanical effect (thick line). Trials 19 and 21, however, began at postures (about 22°) where the difference between the actual movement and the predicted movement was minimal. This match between actual and simulated movement implies that the subject used a torque pattern similar to the pattern used in the simulation (from the CONTROL trial). Subsequently, in trials 23 and 32, the subject gradually adopted a more normal arm path, with the initial posture returning to about 15° (thin lines). To do this without being perturbed by the spin (thick lines), the subject had to alter his pattern of muscular forces.

This series of events seems to represent a two-stage approach to learning the mechanics of the gyro. First the subject gradually changed the initial arm posture from trial to trial; this allowed him to experience a relatively unperturbed movement while using the "normal" pattern of dynamic joint torques. Next, the subject returned to the usual initial posture and made a relatively normal arm movement (see also Figs. 1*C* and 4*C*). With the added torques due to the spin, making the same movement would only be possible by changing self-generated muscular forces.

Analysis of kinetic energy

Another approach to understanding the interaction between the spin and the arm posture comes from an evaluation of mechanical kinetic energy. As mentioned in the introduction, we have previously demonstrated that the kinetic energy of a reaching movement is highly dependent on the arm configuration. We found that for a wide range of speeds, and a given pair of initial and final targets, subjects tended to choose an arm path that minimized the peak kinetic energy (Soechting et al. 1995; Nishikawa et al. 1999). Here, we have taken a similar approach to show that for a given set of joint torques (i.e., the torques from CONTROL trials) and the novel mechanics provided by the spinning gyro, normalized kinetic energy (see METHODS) is a function of initial arm posture. As explained under Methods, we took the torque profiles from the CONTROL trial and applied them to an arm holding a spinning gyro, starting at a range of initial arm postures. Kinetic energy was then computed at the time of peak velocity for each simulated movement.

In Fig. 5*B* (black symbols and dashed lines) the results of the simulation reveal that the relation between normalized kinetic energy and initial arm plane was linear, and reached a low at the most horizontal initial arm planes used by our subjects. In contrast, the data from our subjects (colored symbols and solid arrows) show that the kinetic energy of the actual movements was fairly constant across initial arm posture. On average, the kinetic energy of actual movements matched the simulation at an initial arm plane of about 30–32° (Fig. 5*B*, *left panel*). As presented above in Fig. 4*C*, the average initial arm plane peaked at this "ideal" value of 32° before returning to the normal value of 26°. For subject 1, this ideal, low energy initial posture was at about 22° (Fig. 5*B*, *middle panel*), corresponding to his relatively unperturbed trials (19 and 21) in Fig. 5*A*.

In addition, the *right panel* of Fig. 5*B* illustrates that one of the subjects who did not adapt (subject 8) also exhibited a qualitatively different pattern, in that actual kinetic energies were always higher than simulated kinetic energies, with no clear ideal. Subject 7 (data not shown) followed the pattern of subjects 1–6, but was much more variable.

Since subjects eventually moved away from a kinetically ideal arm geometry (in a process apparently aimed at restoring the normal arm geometry), we were surprised to see that this was accomplished without increasing the normalized kinetic energy. In Fig. 5*B*, the actual energy values are color coded for trial number (red = early, yellow/green = middle, blue = late), as the angle of the initial arm plane decreased. The near-zero slope of this progression shows that the simulated increase in energy for the CONTROL torque pattern (black symbols) was avoided in the course of learning a new torque pattern.

Adapting to an inertial perturbation

Analogous results were obtained in a second experiment, where similar reaching movements were perturbed by attaching a rod to the upper arm to change its inertial characteristics (see METHODS). Figure 6*A* shows the average results from six subjects (A-F) in terms of changes in the inclination of the initial arm plane (changes in arm plane rotation and final arm plane were less consistent across subjects). Although the exact time course varied across subjects, the subjects generally increased and then gradually decreased the inclination of the initial arm plane across the first 30 ROD trials.

Using the same format as used for the gyroscope results, Figs. 6, *B* and *C* show a simulation of the rod's mechanical effect for a representative subject. In contrast to the mechanical effect of the gyroscope, in this case the simulation (Fig. 6*B*, black circles and dotted line) revealed a quadratic relation between initial arm posture and normalized kinetic energy, with a clear low (the "ideal") at an initial arm plane of 21°. By changing the initial arm plane, Subject A experienced this energetically ideal posture shortly after the rod was attached to the arm. Figure 6*C* shows that the subject experienced the ideal posture early (trial 21), went beyond it to experience a reversal in the direction of the mechanical effect (trials 26–31), returned to the ideal posture and the normal torque pattern (trial 36), and then returned to the normal kinematics by adapting his joint torques (trial 41). As in the case of the spinning gyroscope, this was done without increasing kinetic energy (Fig. 6*B*, colored symbols). Examination of the torque profiles (data not shown) suggested that this was accomplished by making subtle changes in timing across the four degrees of freedom, but the exact pattern of change was not consistent across subjects.

Figure 6*A* also shows the lack of a mirror-image aftereffect when the rod was removed from the arm (trials 61–90). This was also the case in preliminary gyro experiments (data not shown) and may be related to the fact that subjects were fully aware that the ROD or SPIN was absent.

DISCUSSION

The results of these experiments suggest a two-stage strategy for learning mechanical properties. First, arm geometry is

subtly manipulated by the subject until an "ideal movement" is experienced. By definition, the ideal movement is the one that is launched from the most energetically efficient initial arm posture. Under our perturbation conditions (SPIN or ROD), the ideal movement was also the one where use of the previously learned (CONTROL or NORM) pattern of joint torques produced a relatively unperturbed movement. In a second stage, this previously learned torque pattern is tailored to the mechanics of the tool or device to return the arm to its normal kinematics. In the sections below we will discuss the neuromuscular implications of this strategy, and then the broader implications of the somewhat unexpected return to the normal arm kinematics.

The adaptation strategy

Perhaps experiencing the "ideal movement" facilitates the learning of the new mechanics. Prior to adopting the ideal initial posture, subjects experienced a mismatch between the desired and the actual movement, which undoubtedly activated proprioceptors and trigged reflexive reactions (e.g., trial 17 in Fig. 5*A*). As shown by the simulations in Figs. 5*A* and 6*C*, subjects' movements were relatively unperturbed when they were initiated from the ideal posture. The somatosensory system is thought to operate by comparing the expected to the actual sensory consequences of motor commands (Prochazka 1989; Nelson 1996; see also Hernandez et al. 2002). The present observation of a gradual reduction in this mismatch may be analogous to learning the shape of a surface by moving along it with a gradual reduction in applied force, thereby gradually reducing the perturbation.

Previous studies (e.g., Shadmehr and Moussavi 2000; Lackner and Dizio 1994) have relied on the aftereffect produced by surprise removal of a perturbation, to demonstrate the changes in motor commands due to learning of a novel mechanics. However in a situation where the learning occurred in a particular context, there were no aftereffects when the subjects switched back to the original context (Cohn et al. 2000, Lackner and Dizio 2000). The nature of the perturbations employed in the present series of experiments precluded the possibility of surprise removal, and the gradual changes in motor commands were instead demonstrated by the simulations (Figs. 5*A* and 6*C*). In preliminary experiments, the termination of the gyroscope charging procedure appeared to constitute an obvious change in context. Furthermore, Fig. 1*C* emphasizes that our subjects had experience with both the fast and the slow spin of the gyro throughout the course of learning, and therefore would not be expected to show a strong aftereffect. The data in Fig. 1*C* also suggest that the slow spin trials may have been analogous to "catch trials" in that the arm plane rotation in these trials eventually became greater than for the control trials. This phenomenon, however, was not as clear in the data from some of the other subjects.

Kawato and colleagues have recently shown that humans learn to deal with unpredictable forces in a particular direction, by selectively increasing arm stiffness along that same direction (Burdet et al. 2001). These investigators also demonstrated that whole-arm stiffness gradually decreases as subjects learn a predictable set of torques (Osu et al. 2002). Since we did not measure stiffness in the present study, it is difficult to comment on this aspect of learning. However, muscle cocontraction for the purpose of increasing joint stiffness, by definition, should not change arm posture. Thus it is hard to imagine that the changes in arm posture observed in the present study were merely a reflection of a strategy aimed at regulating joint stiffness.

The relative importance of various kinematic and kinetic parameters

Studies of motor learning offer a window into the process of neuromuscular control. These studies can probe the nature of the error signal that is used to drive the motor learning and can potentially test whether planning is based on kinematics (movements), kinetics (forces) or both (an issue discussed by Hogan and Flash 1987; Soechting et al. 1995; Nakano et al. 1999; Kakei et al. 1999). In many previous studies, the subject's goal was to move a cursor to a target on a computer monitor by moving the hand in a horizontal plane (e.g., Shadmehr and Mussa-Ivaldi 1994). When a perturbation caused a deviation from the usual hand (and cursor) path, subjects adapted by gradually changing the pattern of muscular forces until the straight path was again achieved. Using this type of paradigm, investigators have shown, for example, that new visual/spatial conditions are learned separately from novel force conditions (Flanagan et al. 1999; Krakauer et al. 1999) and that learning generalizes to new regions of the workspace in the frame of reference of the arm muscles (Shadmehr and Moussavi 2000).

In contrast to previous studies, we measured arm configuration as well as hand path. Somewhat surprisingly, over the course of about 500 reaches, subjects gradually moved back to the arm configuration that was normally associated with a particular set of initial and final targets. This was in spite of the fact that the hand path and the arrival of the hand at the target were not in error. Thus it appears that for reaching, whole-arm kinematics (not just hand path or endpoint error) may be the "error signal" that drives the learning.

Our results may help to resolve an ongoing debate concerning the relative importance of kinematics and kinetics in motor control. In our task, the process of adaptation was essentially implemented by and aimed at controlling whole-arm kinematics. At the same time, however, the ideal arm posture was defined based on minimum kinetic energy (or ease of move-

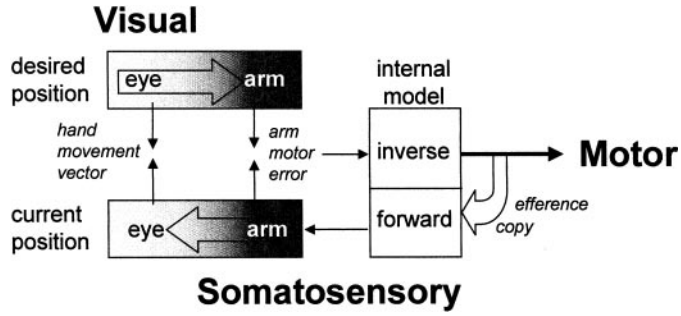

FIG. 7. A hypothetical scenario for sensorimotor control. The Motor output is produced by a moment-by-moment comparison of current and desired arm configuration (*arm motor error*). The arm-centered representation is in the reference frame of the Somatosensory and Motor systems. In situations of Visual guidance, computation of a *hand movement vector* may be in eye-centered coordinates. The arm- and eye-centered representations are drawn along a continuum to suggest that these two frames of reference may be used concurrently.

ment) and kinetic energy was not increased in the course of adaptation. It has proven to be difficult to experimentally dissociate kinematics and kinetics, and it seems plausible that the sensorimotor system is equally concerned with both types of signal.

A model for sensorimotor control

Whereas previous studies have emphasized the kinematics of the hand path, the present results show, for the first time, that subtle changes in whole-arm posture are actively manipulated by the motor system. This observation highlights the importance of body configuration in motor control and is consistent with recent results suggesting that proprioceptors can encode whole-limb geometry, independent of muscle force (Bosco and Poppele 2000). This new evidence is also compatible with a hypothetical scheme in which movements are generated based on a moment by moment comparison of current and desired arm postures (Desmurget and Grafton 2000; Soechting and Flanders 2002).

This hypothetical scheme is illustrated in Fig. 7. The "internal model" is central to the sensorimotor transformation illustrated here, and is presumably central to the process of learning the mechanical properties of hand-held devices (Wolpert et al. 2001). It has two portions. The "inverse model" maps the desired movement kinematics (the hand path or the arm path) into the appropriate muscle forces, or motor commands. The "forward model" uses an efference copy of the motor command to predict the sensory consequences (in terms of arm path or hand path). On the far left of the flow chart, we show that the input to the transformation entails a moment-by-moment comparison between the "current position" and the "desired position." In a task such as drawing a line under visual guidance, this comparison may be in terms of an eye-centered hand movement vector (Buneo et al. 2002). However to generate the proper input to the inverse model, this hand movement vector should be transformed into an arm motor error signal, taking into account the whole-arm configuration. Our present results highlight the fact that current whole-arm configuration is essential for the correct calculation of motor commands, with or without altered arm mechanics.

This work was supported by grant R01 NS-27484 to M. Flanders from the National Institute of Neurological Disorders and Stroke.

REFERENCES

Atkeson CG and Hollerbach JM. Kinematic features of unrestrained vertical arm movements. *J Neurosci* 5: 2318–2330, 1985.

Bosco G and Poppele RE. Reference frames for spinal proprioception: Kinematics based or kinetics based? *J Neurophysiol* 83: 2946–2955, 2000.

Buneo CA, Boline J, Soechting JF, and Poppele RE. On the form of the internal model for reaching. *Exp Brain Res* 104: 467–479, 1995.

Buneo CA, Soechting JF, and Flanders M. Postural dependence of muscle actions: implications for neural control. *J Neurosci* 17: 2128–2142, 1997.

Buneo CA, Jarvis MR, Batista AP, and Andersen RA. Direct visuomotor transformations for reaching. *Nature* 416: 632–636, 2002.

Burdet E, Osu R, Franklin DW, Milner TE, and Kawato M. The central nervous system stabilizes unstable dynamics by learning optimal impedance. *Nature* 414: 446–449, 2001.

Cohn JV, Dizio P, and Lackner JR. Reaching during virtual rotation: Context specific compensation for expected Coriolis forces. *J Neurophysiol* 83: 3230–3240, 2000.

Craig JJ. *Introduction to Robotics: Mechanics and Control*. 2nd Edition. Reading, Massachusetts: Addison-Wesley Publishing Co., Inc., 1989.

Desmurget M and Grafton S. Forward modeling allows feedback control for fast reaching movements. *Trends Cog Sci* 4: 423–431, 2000.

Flanagan RJ, Nakano E, Imamizu H, Osu R, Yoshioka T, and Kawato M. Composition and decomposition of internal models in motor learning under altered kinematic and dynamic environments. *J Neurosci 19:RC* 34: 1–5, 1999.

Ghez C, Gordon J, Ghilardi M-F, Christakos CN, and Cooper SE. Roles of proprioceptive input in the programming of arm trajectories. *Cold Spring Harbor Symp Quant Biol* 55:837–847, 1990.

Hernandez A, Zainos A, and Romo R. Temporal evolution of a decision-making process in medial premotor cortex. *Neuron* 33: 959–972, 2002.

Hogan N and Flash T. Moving gracefully: quantitative theories of motor coordination. *Trends Neurosci* 10: 170–174, 1987.

Kakei S, Hoffman DS, and Strick PL. Muscle and movement representations in primary motor cortex. *Science* 285:2136–2139, 1999.

Krakauer JW, Ghilardi, M-F, and Ghez C. Independent learning of internal models for kinematic and dynamic control of reaching. *Nature Neurosci* 2: 1026–1031, 1999.

Lackner JR and Dizio P. Rapid adaptation to Coriolis force perturbations of arm trajectory. *J Neurophysiol* 72: 299–313, 1994.

Lackner JR and Dizio P. Aspects of body self-calibration. *Trends Cog Sci* 4: 279–288, 2000.

Nakano E, Imamizu H, Osu R, Uno Y, Gomi H, Yoshioka T, and Kawato M. Quantitative examinations of internal representations for arm trajectory planning: minimum commanded torque change model. *J Neurophysiol* 81: 2140–2155, 1999.

Nelson RJ. Interactions between motor commands and somatic perceptions in sensorimotor cortex. *Curr Opinion Neurobiol* 6: 801–810, 1996.

Nishikawa KC, Murray ST, and Flanders M. Do arm postures vary with the speed of reaching? *J Neurophysiol* 81: 2582–2586, 1999.

Osu R, Franklin DW, Kato H, Gomi H, Domen K, Yoshioka T, and Kawato M. Short- and long-term changes in joint co-contraction associated with motor learning as revealed from surface EMG. *J Neurophysiol* 88: 991–1004, 2002.

Prochazka A. Sensorimotor gain control: a basic strategy of motor systems? *Prog Neurobiol* 33: 281–307, 1989.

Shadmehr R and Brashers-Krug T. Functional stages in the formation of human long-term motor memory. *J Neurosci* 17: 409–419, 1997.

Shadmehr R and Moussavi ZMK. Spatial generalization from learning dynamics of reaching movements. *J Neurosci* 20: 7807–7815, 2000.

Shadmehr R and Mussa-Ivaldi FA. Adaptive representation of learning of a motor task. *J Neurosci* 14: 3208–3224, 1994.

Shockley K, Grocki M, Carello C, and Turvey MT. Somatosensory attunment to the rigid body laws. *Exp Brain Res* 136: 133–137, 2001.

Soechting JF and Flanders M. Movement planning: Kinematics, dynamics, both or neither? In: *Vision and action*, eds. L. Harris and M. Jenkin. New York: Cambridge Univ. Press, 1998, p. 352–371.

Soechting JF and Flanders M. Movement regulation. In: *Encyclopedia of the Human Brain, volume 3, ed.* V. S. Ramachandran. San Diego: Academic Press, 2002, p. 201–210.

Soechting JF, Buneo CA, Herrmann U, and Flanders M. Moving effortlessly in three dimensions: Does Donder's Law apply to arm movement? *J Neurosci* 15: 6271–6280, 1995.

Turvey MT, Shockley K, and Carello C. Affordance, proper function, and the physical basis of perceived heaviness. *Cognition* 73: B17–B26, 1999.

Wolpert DM, Ghahramani Z, and Flanagan JR. Perspectives and problems in motor learning. *Trends Cog Sci* 5: 487–494, 2001.